Hierarchical 2D/2D C-$ZnIn_2S_4$/O-PCN S-Scheme Heterojunction for Enhanced Photocatalytic Hydrogen Production

Ping Zhang [1a], Lei Wang[1b], Fangzhou Li[1c], Yuan Liu[1d], Lijun Wu[1e*]

[1]School of Mechanical Engineering, Tongji University, Shanghai 201804, China

Abstract—The heat agglomeration, inadequate optical absorption, significant electron-hole recombination are the main reasons resulting to the low photocatalytic activity of carbon nitride. Herein, based on O-defective functionalized carbon nitride, the C atoms are designed to insert into ZIS lattice to broaden light adsorption intensity and range to near-infrared light (NIR), then are adopted to construct a 2D/2D heterojunction of hierarchical C-$ZnIn_2S_4$/O-PCN nanoflower to enhance the photocatalytic hydrogen evolution of carbon nitride from water splitting. The successful incorporation of C atoms can be revealed by the elemental analysis, enhanced N2 adsorption, and deformation of crystal lattice in C-ZIS. A distinct curve edge of amorphous O-PCN and crystalline C-ZIS, confirm the formation of C-ZIS/O-PCN heterostructures. The optimal matchability is achieved as the mass ratio of C-ZIS to O-PCN is 1:1, which corresponds to the highest photocatalytic hydrogen evolution rate of 1274.8 μmol/g/h, 16.7 times higher than O-PCN. This enhancement is responsible for the largest 2D/2D surface contact, broadened optical adsorption intensity and range, rapid charge transfer at the interface, and the formation of S-Scheme route in the 50%C-ZIS/O-PCN heterojunction.

1. Introduction

The depletion of primary energy and environment crisis have created a growing need for clean regenerated solar sources [1,2]. Photocatalytic water splitting for hydrogen evolution is an ideal approach to convert solar resource into chemical energy[3]. Carbon nitrides are appealing materials due of their excellent properties, including their suitable energy-band for H_2O splitting, superior chemical stability, metal-free composition, and ease of preparation[4]. However, conventional carbon nitrides have several limitations that restrict their photocatalytic H_2 production efficiency. These limitations include low surface-area, inadequate light absorption, limited hydrogen-generated sites, significant electron-hole recombination, and slow carriers transition rate [5]. Addressing these challenges is crucial to enhancing the effective photoelectron yields for carbon nitride and improving its photocatalytic H_2 production efficiency.

Defect engineering is an important method to address above issues. Carbon nitrogen-based defect engineering mainly involves atoms-doping [6,7], lattice vacancies [8], and functional groups [7,9], among which the modification of functional groups plays a vital role due to the controllability of its defect position and defect concentration [10]. However, most of researches on defect carbon nitrides are limited to the employ of Pt noble metal as the cocatalyst. The high cost of Pt is not suitable for actual application. Constructing semiconductor heterojunction is an effective strategy to substitute for Pt to restrain the re-combination of excited electron-hole pairs [11,12].

The dimension of functionalized materials is an important parameter affecting photocatalytic performance [13,14], where 2D nanomaterials typically exhibit high surface-areas, distinctive surface features, and quantum confinement effects [14-16]. $ZnIn_2S_4$ hexagonal phase bimetallic sulfide, due to its efficient visible light absorption, superior stability compared to binary sulfides, and nanoflower morphology with high surface area, has become a widely studied 2D nanomaterial for semiconductor photocatalysis. Herein, C atoms doped ZIS nanoflower structures are designed to expand the optical absorption range to NIR light. Then, based on O-defective functionalized carbon nitride (O-PCN), a 2D/2D heterojunction of C-$ZnIn_2S_4$/O-PCN nanoflower was constructed to enhance the photocatalytic hydrogen evolution of carbon nitride from water splitting. The loading content of 50 wt% C-ZIS on O-PCN achieve the highest photocatalytic hydrogen evolution with a rate of 1274.8 μmol/g/h, which is 16.7 times higher than that of pristine O-PCN. This significant enhancement is responsible by the optimal 2D/2D surface contact, broadened optical adsorption intensity and range,

[a]1810232@tongji.edu.cn; [b]2132729@tongji.edu.cn; [c]2132728@tongji.edu.cn; [d]2111412@tongji.edu.cn; [e*]ljwu@tongji.edu.cn

rapid charge transfer at the interface, and the formation of S-Scheme route in the 50%C-ZIS/O-PCN heterojunction.

2. Experimental sections

2.1 Preparation of materials

The preparation of carbon nitride (PCN) and O-PCN was referenced from previous reports [11]. C-doped $ZnIn_2S_4$, noted as C-ZIS, was synthesized through hydrothermal method: $Zn(Ac)_2 \cdot H_2O$, $InCl_3$, and L-cysteine were added stepwise to 30 mL distilled H_2O in an elemental molar ratio of Zn:In:S = 1:2:4. The resulting mixture was then placed in a autoclave and heated to 180°C for 18 h. The obtained suspension was washed three times with ethanol and distilled H_2O, and the resulting solid was dried under vacuum at 60 °C for 12 h. The preparation of C-ZIS/O-PCN is the same as the above method, except that different contents of O-PCN were added into the 30 mL of deionized H_2O, which were noted as x% C-$ZnIn_2S_4$/O-PCN, and the x value was set as 10%, 30%, 50%, 70%, respectively.

2.2 Characterizations

The morphologies of these materials were examined on a scanning electron microscopy (SEM, S-4800) and a transmission electron microscopy (TEM, JEOL 3200F). X-ray powder diffraction (XRD) was measured using a powder diffractometer of Bruker D8. The N_2 adsorption and desorption was analyzed on Autosorb-iQ-AG equipment. The UV-vis adsorption spectra were tested on SHIMADZU UV-3600 spectrometer. Photoluminescence spectrum (PL) was achieved via Hitachi F-4600 fluorescence spectrophotometer. An electrochemical device of CHI 660E was used for electrochemical characterization. The preparation of working electrode can refer the previous literatures [12].

2.3 Photocatalytic evaluation

The evolutions of photocatalytic hydrogen generation were performed in a glass circulation-system. The results were tested by a gas chromatograph (GC-2010 Plus, SHIMADZU, Japan). Typically, 50 mg of samples were added into 80 mLof distilled H_2O and 20 mL of methanol. A 300 W Xenon-lamp, cut by 1.5 AM filter, was adopted as light source to simulate solar irradiation (Perfectlight, PLSSXE 300C). The detailed operation steps can be found in the previous reports [11].

3. Results and Discussions

3.1 Defective structures and morphologies

Previous studies have confirmed the successful formation of O-defected carbon nitrides[7]. The amorphous structure with planar laminar stacking of pristine PCN is shown in Fig. 1a. Whereas, after modulation with O-functional groups, the O-PCN in Fig. 1b evolves into granular pieces with an average size of 25 nm. This morphological difference provides further evidence of the successful synthesis of O-PCN. Fig.1c displays the 2D hierarchical nanoflower structures of C atoms doped ZIS with an average diameter of 500 nm. According to previous reports on ZIS, the nanoflower-like morphology is not significantly affected by C-doping[16]. The ordered lattice spacing of C-ZIS shown in Fig. 1d is noted as 0.321 nm, attributed to the (102) crystal plane of ZIS [17]. The distorted and aberrated appearance of the atom arrangement at the edge indicates that C-atoms were inserted into the crystal lattice of ZIS, providing intuitive evidence of the doping of C atoms into the ZIS crystalline. The lattice distortion also leads to the creation of more micropores, as evidenced by the increased N_2 adsorption capacity and pore distribution of C-ZIS, compared with ZIS in Fig 2a.

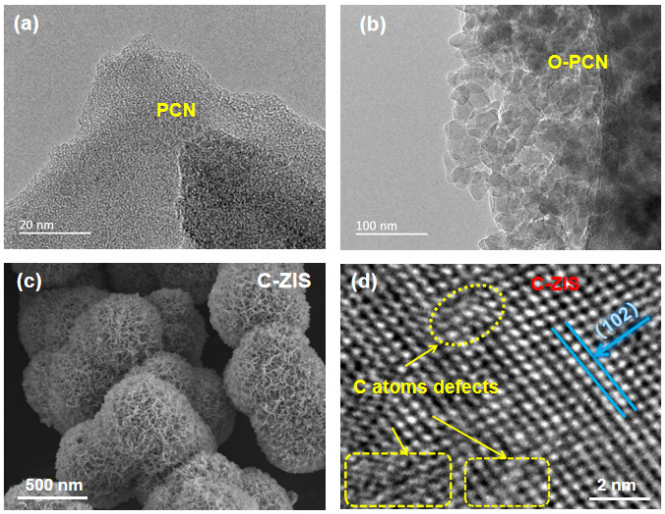

Fig.1 TEM morphologies of PCN (a) and O-PCN (b); SEM images (c) and HR-TEM image (d) of C-ZIS.

To further investigate the amount of C doping in ZIS, the elemental composition of the samples are analyzed, including C, N, O, Zn, In, and S. As shown in Table 1, the C/N atomic ratio for pristine PCN is 1.13, while the C/N ratios for 50%C-ZIS/O-PCN and 50%ZIS/O-PCN are 3.59 and 0.63, respectively. The result indicates that the C content in 50%C-ZIS/O-PCN is 5.6 times higher than that in 50%ZIS/O-PCN, suggesting a significant amount of C atoms were incorporated into the ZIS crystal lattice. Additionally, the chemical stoichiometry of the doped samples became $ZnIn_{1.5}S_3$, and the reduced proportion of S atoms suggests that the doped C atoms may have replaced some of the lattice S positions.

Table 1. The contents analysis of C, N, O, Zn, In, and S elements

Samples	C (at.%)	N (at.%)	O (at.%)	S(at.%)	Zn (at.%)	In (at.%)
O-PCN	50.36	44.6	5.04	0.14	–	–
C-ZIS	52.2	–	8.96	21.7	6.99	10.14
50%C-ZIS/O-PCN	35.16	9.79	6.04	26.45	9.74	12.82
50%ZIS/O-PCN	35.4	37.35	12.42	7.84	2.94	4.05

3.2 Hierarchical 2D/2D heterostructures

XRD results show that with the increase of C-ZIS content in C-ZIS/O-PCN, the intensity of the (002) facet of PCN decreases, demonstrating a reduction in the stacking thickness of CN layers. This suggests that the stacking thickness of CN layer is hindered during the preparation procedure, thus facilitating the coverage of C-ZIS 2D layers on CN granular pieces, and the formation of a more uniform 2D/2D layer stacking. The intensity of the (100) plane remains the same, indicating that the heterostructure formation does not affect the in-plane arrangement of heptazine motifs. According to the JCPDS No.49.1562, the signal at 21.6°, 27.4° and 47.2° are corresponding to (006), (102) and (110) facets [18]. Additionally, 50%C-ZIS/O-PCN has a maximum exposure of the (110) plane, which is identified as the active facet for hydrogen evolution based on DFT calculations [19].

50%C-ZIS/O-PCN maintains their nanoflower morphology with slight depressional deformation, as depicted in Fig. 2c. This change may indicate a strong force between C-ZIS and O-PCN. The absence of distinct isolated O-PCN particles suggests that the hydrothermal procedure exfoliated O-PCN nanoparticles into thin nanolayers, promoting their full contact with C-ZIS precursors and uniform distribution of these two types of layers at the composite interface. Figure 2d displays the distinct curve edge of amorphous O-PCN and crystalline C-ZIS, verifying the formation of C-ZIS/O-PCN heterostructures. The overlaying of C-ZIS lattice fringe on the amorphous O-PCN further confirms the 2D/2D surface contact mode, maximizing the interface contact area and facilitating the rapid transmission of charge at the interface of the two semiconductors.

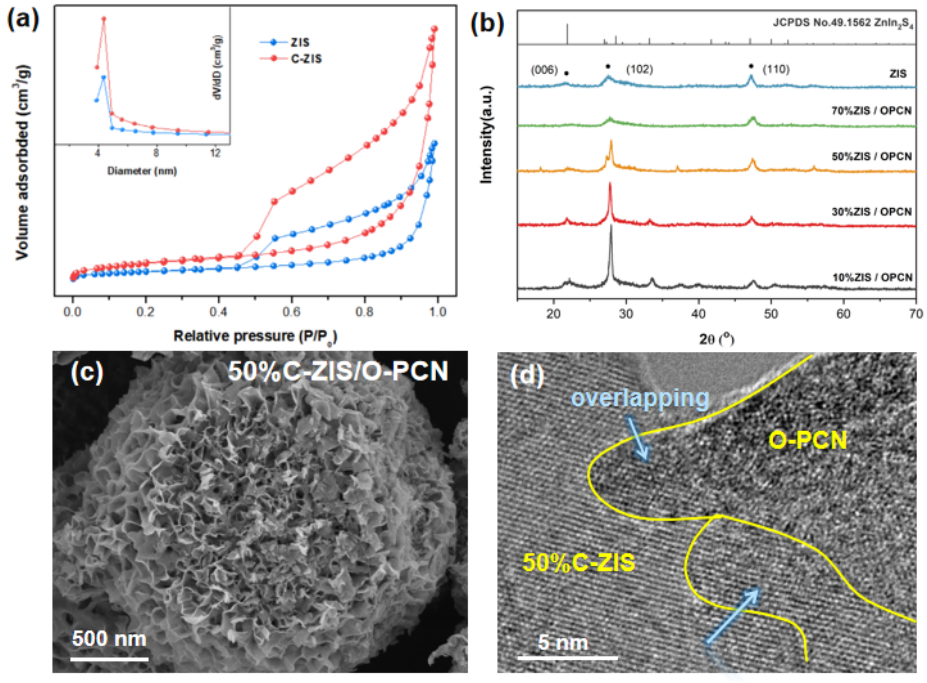

Fig. 2 N_2 adsorption-desorption of ZIS and C-ZIS (a); XRD patterns (b); SEM image (c) and HR-TEM image (d) of 50%C-ZIS/O-PCN.

3.3 Evolution of photocatalytic activity

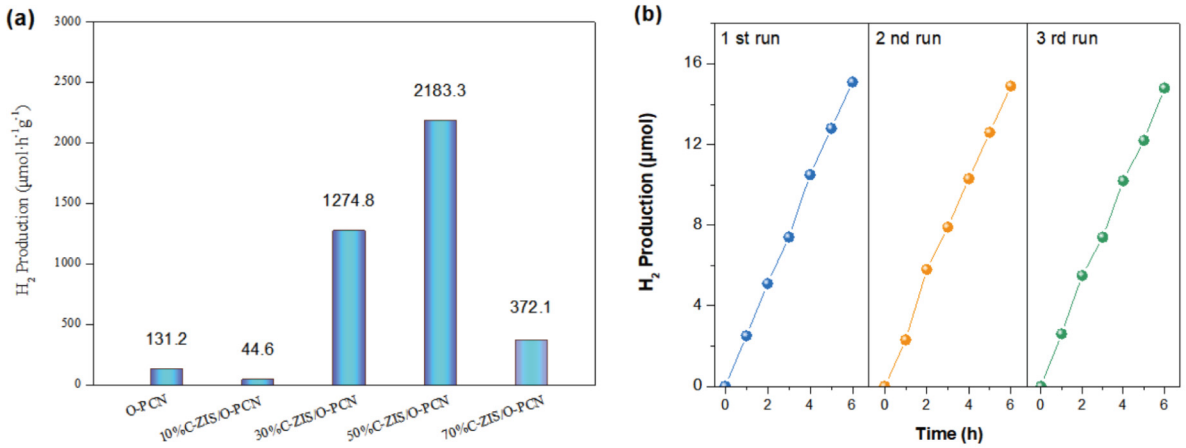

Fig. 3 H_2 evolution rate of the C-ZIS/O-PCN with different C-ZIS contents (a) and the cycle tests of 50%C-ZIS/O-PCN (b).

Fig. 3a shows the photocatalytic hydrogen activity of composites with different amounts of ZIS. The results indicate an increasing trend followed by a decrease as the amount of C-ZIS increases. The highest H_2 yield rate of 1274.8 μmol/h/g is observed for the composite with 50 wt% C-ZIS loading on O-PCN, which is 16.7 times higher than that of O-PCN alone. This suggests that the optimal matchability of the heterogeneous structures is obtained as the mass ratio of C-ZIS to O-PCN is 1:1, which is likely due to the optimal 2D/2D surface contact of 50wt% C-ZIS on O-PCN. However, the activity of the composite with 10 wt% C-ZIS loading is lower than that of O-PCN, possibly due to the shielding effect of C-ZIS on the active sites of O-PCN. Further increases in C-ZIS loading lead to a decreased H_2 yield, possibly due to the deterioration of matchability. Fig. 3b shows that the 50%C-ZIS/O-PCN composite maintains a high H_2 production rate after three-cycles of tests.

3.4 Evolution of photocatalytic activity

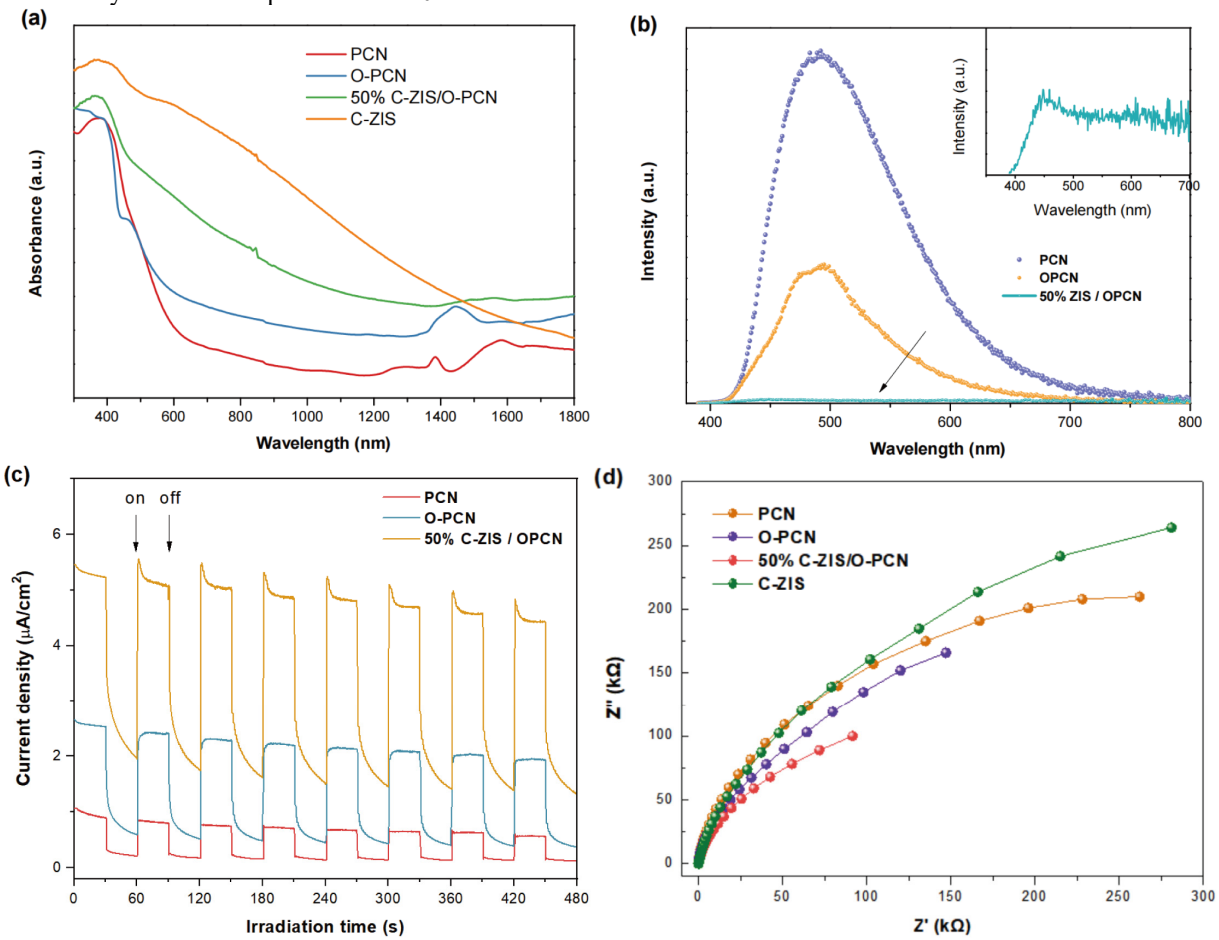

Fig.4 UV-vis adsorption spectra (a), PL spactra (b), photocurrent (c), and electrochemical impedance (d).

3.5 Band Energy

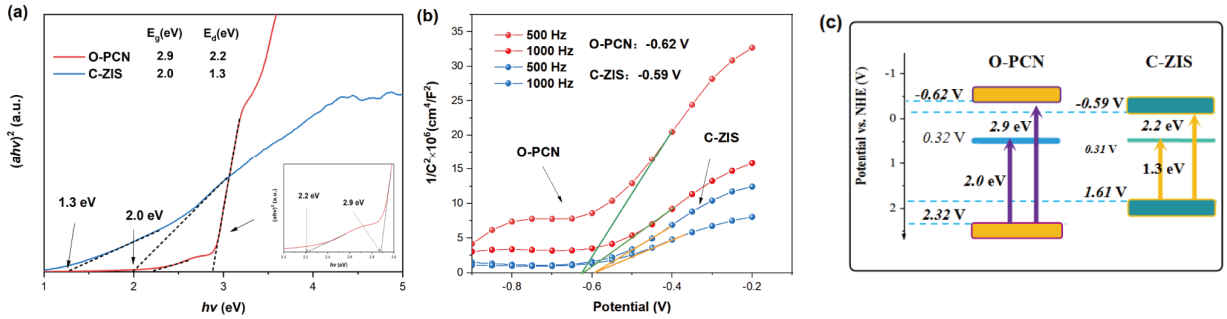

Fig. 5 Tauc plots (a), Mott-Schottky curves (b), and energy bands (c).

To investigate the direction and mechanism of charge transfer at the interface, we analyzed the energy bands of O-PCN and C-ZIS by examining band gaps and flat band potentials. The Tauc plots indicated that the band gap of O-PCN and C-ZIS are 2.9 eV and 2.0 eV, with the midgap of 2.2 eV and 1.3 eV, respectively. The deceased band gap of C-ZIS is caused by the C-doping. Based on the Mott-Schottky results, the flat potentials are -0.62 V and -0.59 V (vs. Ag/AgCl electrode), respectively, which satisfy the requirement for H_2 generation. The calculated band arrangements of O-PCN and C-ZIS are illustrated in Fig. 5(c). For O-PCN, the actual electronic potential should be the trapped state potential. Under light irradiation, the active electrons trapped on the surface of O-PCN will move to the valence band of C-ZIS to recombine with the holes driven by the potential difference, then jump to the conduction band. This S-Scheme charge transfer in 50%C-ZIS/O-PCN is not only conducive to the separation of electron-hole pairs to produce H_2, but also maintain the high reduction capability due to the negative potential.

4. Conclusion

The C atoms are designed to insert into ZIS lattice to broaden light adsorption range to near-infrared light. The successful incorporation can be revealed by the elemental analysis, enhanced N_2 adsorption, and deformation of crystal lattice in C-ZIS. The C-doping also enables C-ZIS to absorb the entire range of light wavelength with high intensities in visible and near-infrared regions. Furthermore, based on O-defective functionalized carbon nitride, a 2D/2D heterojunction of C-$ZnIn_2S_4$/O-PCN nanoflower is constructed to enhance the photocatalytic H_2 yield of carbon nitride from water splitting. A distinct curve edge of amorphous O-PCN and crystalline C-ZIS, verifies the formation of C-ZIS/O-PCN heterostructures. The optimal matchability is obtained as the mass ratio of C-ZIS to O-PCN is 1:1, which corresponds to the highest photocatalytic hydrogen evolution rate of 1274.8 μmol/g/h, 16.7 times higher than O-PCN. The enhancement is responsible for the largest 2D/2D surface contact, broadened optical adsorption intensity and range, rapid charge transfer at the interface, and the formation of S-Scheme route in the 50%C-ZIS/O-PCN heterojunction.

Acknowledgments

This work was supported by the China Scholarship Council and Chat GPT.

References

1. Wang C., Liu X., He W., et al. (2020), J. Catal., 389: 440-449.
2. Zhang P., Pan W. g., Guo R. t., et al. (2019), J. Energy Inst., 92(5): 1313-1328.
3. Wang L., Hong Y., Liu E., et al. (2020), Carbon, 163: 234-243.
4. Huang Z., Zhang Y., Dai H., et al. (2019), J. Catal., 378: 331-340.
5. Wang X., Maeda K., Thomas A., et al. (2009), Nat. Mat., 8(1): 76-80.
6. Zhao D., Dong C.-L., Bin W., et al. (2019), Adv. Mat., 31(43): 1903545.
7. Lau V. W. h., Yu V. W. z., Ehrat F., et al. (2017), Adv. Energy Mat, 7(12): 1602251.
8. Zhang P., Wu L.-J., Pan W.-G., et al. (2021), Solar RRL, 5(3): 2000796.
9. Dong G., Jacobs D. L., Zang L., et al. (2017), Appl. Catal. B Environ., 218: 515-524.
10. Lau V. W.-h., Moudrakovski I., Botari T., et al. (2016), Nat. Commun., 7: 12165.
11. Zhang P., Wu L.-j., Pan W.-g., et al. (2021), Appl. Catal. B Environ., 289: 120040.
12. Zhang P., Guo R.-t., Wu L.-j., et al. (2021), Appl. Surf. Sci., 542: 148707.
13. Zuo G., Wang Y., Teo W. L., et al. (2020), Angew. Chem., 132(28): 11383-11388.
14. Chen Y., Fan Z., Zhang Z., et al. (2018), Chem. Rev., 118(13): 6409-6455.
15. Meng L., He J., Zhou X., et al. (2021), Nat. Commun., 12(1): 1-9.
16. Zhou M., Liu Z., Song Q., et al. (2019), Appl Catal B: Environ, 244: 188-196.
17. Du C., Zhang Q., Lin Z., et al. (2019), Appl. Catal. B Environ., 248: 193-201.
18. Wang S., Guan B. Y., Lou X. W. D. (2018), J. Am. Chem. Soc., 140(15): 5037-5040.

19. Shi X., Mao L., Yang P., et al. (2020), Appl. Catal. B Environ., 265: 118616.